

Formation and propagation of spin-wave envelope solitons in weakly dissipative ferrite waveguides

A. N. Slavin

Department of Physics, Oakland University, Rochester, Michigan 48309

H. Benner

Institut für Festkörperphysik, Technische Universität Darmstadt, D-64289 Darmstadt, Germany

(Received 8 October 2002; revised manuscript received 31 January 2003; published 28 May 2003)

The influence of dissipation on the process of formation and propagation of envelope solitons is considered on the example of spin wave envelope solitons in yttrium iron garnet (YIG) film waveguides. It is shown that the measurements of attenuation of the peak power of a propagating nonlinear wave packet in a weakly dissipative medium can be used to determine the soliton formation length. This length turns out to be smaller than the characteristic dispersion length calculated for a given shape and duration of the input pulse. A simple approximate analytic expression for the soliton formation time in a dissipative medium is introduced and confirmed by both numerical calculations and preliminary laboratory experiments on dipolar spin waves in YIG waveguides.

DOI: 10.1103/PhysRevB.67.174421

PACS number(s): 75.30.Ds, 76.50.+g, 85.70.Ge

I. INTRODUCTION

Envelope solitons are stable nonlinear wave packets that preserve their shape while propagating in a nonlinear dispersive medium, even after collisions with other envelope solitons. These properties make them attractive for applications as information carriers in communication and signal processing systems. In particular, optical envelope solitons in fibers have been studied very intensively during recent decades (see Ref. 1 and references therein). These optical solitons propagating in silica fibers with very low propagation losses have a typical duration of several picoseconds, and are considered now as the most promising carriers of information in future fiber optic communication lines.²

Another important example of a physical system where envelope solitons can be easily observed and studied experimentally are spin waves propagating in thin magnetic films.³ Spin-wave envelope solitons propagating in yttrium iron garnet (YIG) films typically have carrier frequencies in the microwave frequency range (i.e., several gigahertz), a group velocity about four orders of magnitude smaller than the group velocity of optical solitons and durations of 5–200 ns. Solitons of this type might find applications in microwave signal processing systems and radar technology.⁴

In all laboratory experiments where envelope solitons have been studied, they were propagating in media with weak, but finite dissipation. Of course, in all the “soliton” experiments (in optical fibers,^{1,2} magnetic films,³ on the water surface, and in other physical systems⁵), special care was taken to make sure that the influence of dissipation on the profile of the propagating wave pulse is small compared to competing influences of dispersion and nonlinearity that are responsible for the soliton formation. However, the influence of dissipation cannot completely be excluded, and therefore the experimentally observed nonlinear wave packets are not envelope solitons in a pure mathematical sense of this definition.⁶ In every medium supporting envelope solitons there is, however, an interval of propagation distances in which the propagating nonlinear wave packet has “solitonic”

properties (i.e., approximately preserves its shape in propagation and in collisions with other solitons). This interval is limited from below, because it takes a certain minimum propagation length to form a soliton from an arbitrary input pulse. It is also limited from above, because at large propagation distances in a dissipative medium the amplitude of a propagating wave packet decreases (as, consequently, does the influence of nonlinearity) and, finally, the dissipation and the unbalanced effect of dispersion lead to the destruction of a soliton. These “approximately solitonic” nonlinear wave packets moving in the above described limited interval of propagation distances we shall call “envelope solitons” below. It also turns out that in some media dissipation can play a decisive role in the formation process of envelope solitons from initially linear wave pulses when their amplitude is increased, and can determine the shape of the threshold curve for soliton formation.

We have chosen magnetic (or spin wave) envelope solitons for this study because they are much stronger affected by dissipation than, e.g., optical solitons in fibers. Even the best magnetic materials (monocrystalline YIG films) have relaxation parameters that are three orders of magnitude larger than the corresponding parameters in optical fibers. Spin waves in magnetic films are also relatively slow (four orders of magnitude slower than optical waves in fibers), which leads to a much larger spatial attenuation and propagation losses of spin waves. Thus, the influence of dissipation is critical and has to be taken into account in the case of spin-wave envelope solitons.

The aim of this paper is to study the influence of dissipation on the process of formation and propagation of envelope solitons in nonlinear dispersive media. Using the example of spin-wave envelope solitons, we show that the dissipation parameter in a weakly dissipative medium determines the amplitude threshold of the envelope soliton formation. It also determines the shape and fine structure of the threshold curve, and the optimum duration of the input wave pulses for which the threshold of envelope soliton formation has minima. We show that it is reasonable to use measurements

TABLE I. Characteristic parameters in optical and magnetic media.

Type of waves	$ v_g $ (cm/s)	$ D $ (cm ² /s)	$ N C$ (W ⁻¹ s ⁻¹)	Γ (s ⁻¹)	T (ns)	T_P (μ s)	T_D (μ s)	T_Γ (μ s)
Optical waves in single-mode fibers ^a	2×10^{10}	1×10^3	$(0.4-6) \times 10^6$	1×10^4	0.01	5-50	1	100
Magnetostatic waves in YIG films ^{b, c}	4×10^6	3×10^3	1×10^7	5×10^6	20	0.2	0.2	0.2
Dipole-exchange spin waves in YIG films ^{b, d}	2×10^6	5×10^5	3×10^7	5×10^6	200	0.2	0.05	0.2

^aReference 1.^bReference 3.^cReference 10.^dReference 15.

of the peak power attenuation of a nonlinear wave packet propagating in a weakly dissipative medium to determine experimentally the propagation length L_f , within which the soliton is formed, and the interval of propagation distances L_s where the propagating wave packet retains its solitonic properties.

II. EVOLUTION EQUATION

Below we shall restrict our attention to the case of quasi-one-dimensional spin-wave soliton propagation in narrow strips of YIG films (YIG waveguides), having a typical width of 1–2 mm. Diffraction, self-focusing, and other two-dimensional effects, which manifest themselves in wider film samples, have been discussed in detail elsewhere.^{7,8} The one-dimensional propagation of envelope solitons in a nonlinear dispersive medium with weak dissipation is usually described by a perturbed nonlinear Schrödinger equation¹⁻³ (NSE) (see also Refs. 9–25),

$$i \left(\frac{\partial \phi}{\partial t} + v_g \frac{\partial \phi}{\partial z} \right) + \frac{D}{2} \frac{\partial^2 \phi}{\partial z^2} - N |\phi|^2 \phi = -i \Gamma \phi, \quad (1)$$

where $\phi(z, t) = \psi(z, t) e^{i\sigma(z, t)}$ is the slowly varying dimensionless complex amplitude of the wave and ψ and σ are real functions. In the case of spin waves propagating in a magnetic medium the complex wave amplitude ϕ is related with the amplitude of transverse magnetization m and saturation magnetization M_0 by³ $\phi^2 = m^2 / 2M_0^2$. In Eq. (1) $v_g = \partial \omega / \partial k|_{k_0}$ is the group velocity, $D = \partial^2 \omega / \partial k^2|_{k_0}$ is the dispersion coefficient, and $N = \partial \omega / \partial |\phi|^2|_{k_0}$ is the nonlinearity coefficient. All coefficients are calculated at the carrier wave number k_0 . The dissipation coefficient $\Gamma = \gamma \Delta H$ is proportional to the ferromagnetic resonance linewidth ΔH of the ferrite and γ denotes the gyromagnetic ratio. The dissipation, which is responsible for the effects of interest in the present paper, is assumed to be a small perturbation compared to all other terms. Typical values of these coefficients, both for

magnetostatic wave soliton experiments in YIG films and for optical envelope solitons in fibers, are given in Table I.

For a lossless medium ($\Gamma = 0$) Eq. (1) was solved exactly using the method of inverse scattering transformation (IST).^{6,19} It was shown that if the Lighthill criterion ($ND < 0$; see Refs. 6 and 9) is fulfilled, the NSE-governed evolution of a sufficiently smooth and rapidly decaying input pulse profile $\phi(z, 0) = U g(z)$ (where U is a real constant) leads to the formation of bright envelope solitons.

The IST method also allows us to find the threshold for the soliton formation. In particular, it was shown in Ref. 6 that in a medium without dissipation a *rectangular* input pulse of duration T and amplitude U splits into n envelope solitons if the following condition is fulfilled:

$$U |v_g| T \sqrt{|N/D|} \geq \frac{\pi(2n-1)}{2}. \quad (2)$$

This condition results from the fact that the linear scattering problem associated with the NSE has n discrete eigenvalues only when the dimensionless area $S = U |v_g| T \sqrt{|N/D|}$ under the rectangular input pulse (which determines the initial scattering potential of the inverse scattering problem) is larger than a minimum value determined by Eq. (2).

The condition (2) gives the threshold amplitude of an input *rectangular* pulse that is required to form n envelope solitons in a medium without dissipation:

$$|N| U_{th}^2 = \frac{1}{4} |D| \left[\frac{(2n-1)\pi}{|v_g| T} \right]^2. \quad (3)$$

It is clear from Eq. (3) that the threshold power for the soliton formation,

$$P_{th} = \frac{U_{th}^2}{C} \quad (4)$$

(where C is a scaling coefficient depending on the efficiency of the MSW excitation and measured in W^{-1}), is inversely proportional to the squared duration of the input pulse. It is also clear that $(2n-1)^2$ times more power is required to form n envelope solitons than to form a single one. As will be shown later, the dissipation in the medium changes the dependence (3) qualitatively (see also Refs. 24 and 26).

III. CHARACTERISTIC LENGTHS AND TIMES: INFLUENCE OF THE SHAPE OF THE INPUT PULSE

Formation and propagation of solitons in the framework of the NSE (1) where dissipation is neglected ($\Gamma=0$) are usually discussed in terms of the characteristic dispersion and nonlinear lengths L_D and L_{NL} (or times $T_D=L_D/|v_g|$ and $T_{NL}=L_{NL}/|v_g|$), which are defined as propagation distances (or time intervals) at which dispersion and nonlinearity in the medium significantly (in some sense) affect the profile of the input wave packet (see, e.g., Refs. 1, 10 and 11), and usually it is considered that the dispersion length is a good estimate of a propagation distance at which a soliton is formed. For example, in optics these lengths are defined as (see Ref. 1, p. 61)

$$L_D = |v_g| T_D = \frac{|v_g|^3 T_0^2}{|D|}, \quad (5)$$

$$L_{NL} = |v_g| T_{NL} = \frac{|v_g|}{|N| U^2}, \quad (6)$$

where T_0 is a parameter characterizing the time duration of the input wave packet. The characteristic lengths in Eqs. (5) and (6) are defined in such a way that the integer part of the square root of their ratio is equal to the order of the soliton solution of the NSE (1) (or ‘‘soliton order’’) N_S (see pp. 142–146 in Ref. 1):

$$N_S = \langle \sqrt{L_D/L_{NL}} \rangle, \quad (7)$$

where $\langle \dots \rangle$ denotes an integer part of the argument. These definitions in optics are used for input pulses of arbitrary but smooth shape.¹

It is, however, intuitively obvious that the input pulses of different shape will be affected differently by the same dispersion, and, therefore, the characteristic dispersion length L_D should depend on the input pulse shape. Also, the parameter T_0 , characterizing the time duration of the input wave packet should be explicitly defined for input pulses of different shapes.

Using the formalism of the inverse scattering problem^{6,12,13,19} we extend the definition (5) of the dispersion length L_D to account for the shape of the input pulse. If we assume that the envelope of the input pulse (at $t=0$) is positive and smooth, $\phi(z,0) = U g(z) > 0$ [$0 < g(z) \leq 1$], the order N_S of the soliton solution of Eq. (1) that develops from an input wave packet of the normalized area S can be found from the expression^{12,13}

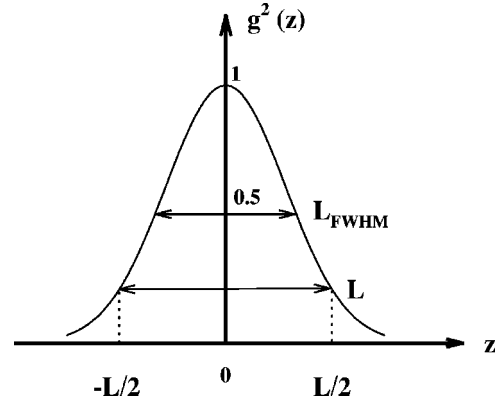


FIG. 1. Intensity profile of the input pulse from which envelope solitons are formed. L is the characteristic width of the pulse defined by Eqs. (12)–(14), while L_{FWHM} is the full width of the pulse at half its maximum of intensity.

$$N_S = \left\langle \frac{S}{\pi} \right\rangle, \quad (8)$$

where $\langle \dots \rangle$ again denotes an integer part of the argument,

$$S = \frac{UL}{\beta} \sqrt{|N/D|} \quad (9)$$

is the dimensionless area under the input pulse, $L=|v_g|T$ and T are the spatial size and the temporal duration of the input pulse, correspondingly, while the dimensionless shape factor β is defined by

$$\beta^{-1} = \frac{1}{L} \int_{-\infty}^{+\infty} g(z) dz, \quad (10)$$

where the function $g^2(z)$ describing the *intensity* (or power) profile of the input pulse is shown in Fig. 1. Condition (8) is a direct generalization of Eq. (2) for the case of an arbitrary smooth shape of the input pulse.^{12,13}

Direct comparison between Eqs. (2) and (8) allows us to find a simple relation between the ‘‘order of soliton solution’’ of Eq. (1) and the ‘‘effective number of solitons’’ n_{eff} ,

$$n_{\text{eff}} = N_S + \frac{1}{2}, \quad (11)$$

which means that for a fundamental (single) soliton solution of the order $N_S=1$ the effective value of n is $n_{\text{eff}}=3/2$. In other words, the fundamental (single) soliton solution of the order $N_S=1$ exists when the dimensionless area of the input pulse lies between the limits defined by Eq. (2) for $n=1$ and $n=2$

$$\frac{\pi}{2} \geq S \geq \frac{3\pi}{2}$$

and the exact single-soliton regime is achieved in the middle of the interval when $S=\pi$ and $n_{\text{eff}}=3/2$. This is illustrated by Fig. 2 where we plot the amplitude U of the input pulse as a function of its inverse width $1/L$ for the simplest case of a rectangular input profile ($\beta=1$). The solid straight lines,

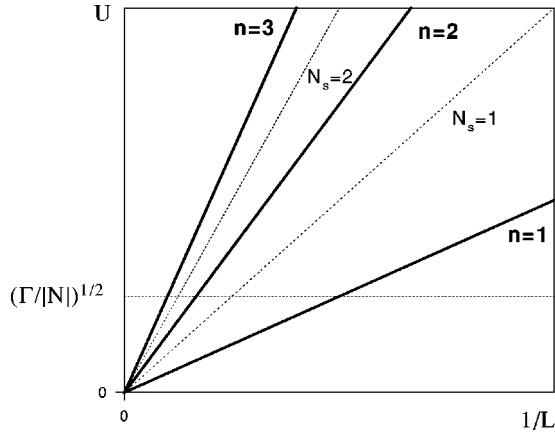


FIG. 2. Regions of existence of n -soliton solutions of the nonlinear Schrödinger equation (1) on the plane “amplitude-inverse length” of the rectangular input pulse.

calculated from Eq. (2), show the boundaries between soliton solutions of different orders N_S , while the inclined broken lines in between, calculated from Eq. (8), correspond to the exact conditions of existence of these solutions. It is clear from Fig. 2 that for any given width L of the input pulse there is a range of amplitudes (between the solid lines corresponding to $n=1$ and $n=2$) where a single (fundamental) soliton $N_S=1$ can exist in the case without dissipation.

The horizontal broken line in Fig. 2 corresponds to the minimum dissipation-dependent threshold of the soliton formation and will be discussed below [see Eqs. (23) and (25)]. It has been shown in Ref. 24 that the presence of dissipation in the medium will restrict from below the interval of input amplitudes in which the formation of a single (fundamental) soliton is possible.

Equation (8) can easily be rewritten in a form similar to Eq. (7) if we retain the definition (6) for the nonlinear length L_{NL} and introduce the following definition for the dispersion length

$$L_D = |v_g|T_D = \frac{|v_g|L^2}{\beta^2 \pi^2 |D|} = \frac{|v_g|^3 T^2}{\beta^2 \pi^2 |D|}, \quad (12)$$

where the shape factor β can be calculated for different input pulse profiles from Eq. (10). In particular, for a rectangular input pulse defined by

$$g(z) = \text{rect}(2z/L) = \begin{cases} 1, & \text{if } |z| \leq L/2 \\ 0, & \text{if } |z| > L/2 \end{cases} \quad (13)$$

the calculation is trivial and yields $\beta=1$. For a Gaussian input pulse

$$g(z) = \exp[-2(z/L)^2], \quad (14)$$

which is widely used in experiments in optical fibers, we have $\beta = \sqrt{2/\pi}$, and the spatial size of the input pulse L is related to the traditionally used “full width at half maximum intensity” L_{FWHM} by $L_{FWHM} = \sqrt{\ln 2}L \approx 0.833L$. For a hyperbolic-secant input pulse,

$$g(z) = \text{sech}[2z/L], \quad (15)$$

we have $\beta = 2/\pi$, and the spatial size of the input pulse $L = |v_g|T$ is related to the width by $L_{FWHM} = [\ln(1+\sqrt{2})]L \approx 0.88L$. The intensity profile of the initial pulse $g^2(z)$ and its parameters L and L_{FWHM} are shown in Fig. 1.

From the comparison of Eqs. (5) and (12) it is clear that the conventional definition¹ of L_D , Eq. (5), is only exact for the hyperbolic-secant input pulse if we assume that the parameter T_0 in Eq. (5) is *half the duration of the input pulse* $T_0 = T/2 = (L/2)|v_g|$. It is also clear from Eq. (12) that the characteristic dispersion time for a rectangular input pulse is considerably $[(\pi/2)^2 \text{ times}]$ shorter than for a hyperbolic-secant pulse of the same duration T . In experiments on optical fiber solitons, where the input pulse duration is relatively short (several picoseconds), and the pulse shape is usually close to either hyperbolic-secant or Gaussian shape, the traditional definitions, Eqs. (5)–(7) work reasonably well when $T_0 = T/2$. In contrast, in spin-wave soliton experiments^{3,10,15–18} the input pulses are relatively long (10–1000 ns) and almost rectangular ($\beta=1$). This fact should be taken into account when calculating the characteristic lengths for spin wave envelope soliton formation, and the definition, Eq. (12), for L_D should be used, especially when the expected “soliton order” N_S is evaluated from these calculations (see, e.g., Ref. 11).

Equation (7) can be rewritten as a threshold condition for the amplitude U of the input pulse of an arbitrary smooth shape having a duration T that is necessary to form n envelope solitons in a medium without dissipation,

$$|N|U_{th}^2 = \frac{1}{4}|D| \left[\frac{\beta\pi(2n-1)}{|v_g|T} \right]^2 = \frac{1}{4}|D|\kappa_n^2, \quad (16)$$

where κ_n is a quantity that has the dimension of inverse length and can be interpreted as a characteristic wave number of the envelope of the input pulse and which depends on the number n of formed solitons:

$$\kappa_n = \frac{\beta\pi(2n-1)}{|v_g|T}, \quad n = 1, 2, 3, \dots \quad (17)$$

IV. INFLUENCE OF DISSIPATION ON THE PROPAGATION OF A SINGLE (FUNDAMENTAL) ENVELOPE SOLITON

When finite but small dissipation is taken into account in Eq. (1), the fundamental “single-soliton” ($N_S=1$) solution of this equation can be found using the perturbation theory, where the dissipative term in the right-hand part of the equation is treated as a small perturbation.¹⁴

The modulus of a single-soliton solution of Eq. (1) obtained for the initial condition

$$\phi(z, 0) = Ug(z)\exp(i\eta z) \quad (18)$$

containing a spatial modulation of the initial profile with wave number η has the form

$$|\phi(z, t)| = Ue^{-2\Gamma t} \text{sech}[Ue^{-2\Gamma t} \sqrt{|N/D|}(z - v_s t)], \quad (19)$$

where the soliton velocity is $v_s = v_g + \eta|D|$. It is clear from Eq. (19) that a small dissipative perturbation does not qualitatively change the single-soliton solution of the NSE without dissipation ($\Gamma=0$). A fully formed envelope soliton simply broadens due to dissipation, and its amplitude decreases with propagation time twice as fast as the amplitude of a linear sinusoidal signal in the same medium. Numerical calculations²⁰ show that the perturbation solution, Eq. (19), works well up to the times $t \leq 0.7\Gamma^{-1}$. Beyond this value the broadening of the propagating soliton changes over to that of a linear pulse and becomes much slower than predicted by the solution, Eq. (19).

In a dissipative medium it is convenient to introduce two more characteristic times for soliton propagation. First of all we shall introduce the characteristic relaxation time in the medium

$$T_\Gamma = \Gamma^{-1}. \quad (20)$$

Another important characteristic time for the soliton formation is the propagation time in the medium T_P , which is equal to the ratio of the propagation distance l and group velocity v_g :

$$T_P = l/|v_g|. \quad (21)$$

In order to observe the formation of envelope solitons (e.g., fundamental $N_S=1$ envelope solitons) in real experiments the characteristic times our system have to fulfill the following relations:¹⁵

$$T_D \ll T_\Gamma, \quad T_N \ll T_\Gamma, \quad T_D \approx T_N, \quad T_N \ll T_P < T_\Gamma. \quad (22)$$

Typical values of some important parameters and characteristics times for optical waves in fibers, magnetostatic waves (or dipolar spin waves), and dipole-exchange spin waves in ferrite films are presented in Table I. It is evident from these values that the influence of dissipation on the process of soliton formation and propagation is much stronger for magnetic solitons than for solitons in optical fibers. Solitons of dipole-dominated spin waves (or magnetostatic waves) are actually formed in a regime, where the influence of dissipation and dispersion on the profile of the input pulse are comparable: $T_D \approx T_\Gamma \approx T_P$, and one may doubt whether nonlinear spin wave packets formed in this regime have solitonic properties. Several recent experiments^{16–18} have shown, however, that nonlinear wave packets formed in this strongly dissipative regime approximately preserve their shapes during propagation and after collisions with other packets, and, therefore, can be called solitons.

Experimental measurements of the effects of dissipation on the propagation of dipolar spin-wave envelope solitons in YIG films^{21,22} have shown that although dissipation for these waves is not a small perturbation (see Table I), the perturbative solution, Eq. (19), describes the expected soliton properties surprisingly well. There is a range of propagation distances within which the dissipation of solitons is exponential and almost twice as large as the dissipation of linear sinusoidal signals in the same medium. This factor 2 in the peak power dissipation rate can be used as a signature of a fully formed soliton in a dissipative medium.

V. INFLUENCE OF DISSIPATION ON THE THRESHOLD AND CHARACTERISTIC TIME OF SOLITON FORMATION

Experiments performed on optical solitons in fibers,^{1,2} where the influence of dissipation is relatively small, have demonstrated that the soliton threshold formulas, Eqs. (3) and (16), obtained in the lossless case ($\Gamma=0$) describe the experiments quite well. The situation was, however, quite different in the case of dipolar spin waves [backward volume magnetostatic waves (BVMSW)] in YIG films where the influence of dissipation is relatively strong.²³ Although the threshold curve measured in Ref. 23 had linear regions with slopes well described by Eq. (3) for $n=1,2$, it also had a distinct structure with two well-pronounced minima that were not described by the classical theory, Eq. (3). The explanation for this threshold curve was given in Ref. 24 where dissipation was taken into account in the process of envelope soliton formation.

The threshold formula derived in Ref. 24 using formalism²⁵ has the form

$$|N|U_{th n}^2 = \frac{\Gamma^2 + \frac{1}{4}D^2\kappa_n^4}{|D|\kappa_n^2}, \quad (23)$$

where κ_n is defined by Eq. (17). The right-hand-side part of the threshold condition, Eq. (23), defines a series of threshold curves corresponding to the formation of $n=1,2,3,\dots$ envelope solitons. These curves have minima at $T=T_n$ which are given by the expression

$$T_n = \frac{\pi\beta(2n-1)}{|v_g|} \sqrt{\frac{|D|}{2\Gamma}}. \quad (24)$$

Thus, in a weakly dissipative medium there is an optimum duration of an input pulse $T=T_n$ which corresponds to a minimum threshold of the formation of n envelope solitons defined by the expression

$$|N|U_{th min}^2 = \Gamma. \quad (25)$$

The threshold curves calculated from Eq. (23) for the rectangular input pulse ($\beta=1$) and $n=1,2,3$ are shown in Fig. 3 of Ref. 24. Note that by means of Eqs. (23)–(25) the expression for the relative threshold of soliton formation in a dissipative medium can be written in the simple normalized form

$$\frac{U_{th n}^2}{U_{th min}^2} = \frac{1 + (T_n/T)^4}{2(T_n/T)^2}. \quad (26)$$

It is interesting to note that Eq. (23) can also be rewritten [similar to Eq. (2)] as a threshold condition for the dimensionless pulse area S defined by Eq. (9):

$$S_{th n} = \frac{\pi(2n-1)}{2} \sqrt{1 + \left(\frac{2\Gamma}{|D|\kappa_n^2}\right)^2}. \quad (27)$$

It follows from Eq. (27) that for the conditions of the experiments^{23,26} only the threshold area necessary for the formation of a single ($n=1$) soliton is substantially cor-

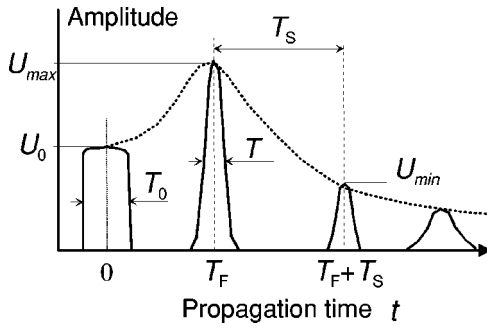


FIG. 3. Schematic picture showing evolution of an input pulse of duration T_0 and amplitude U_0 in a nonlinear dispersive medium with dissipation. T_F is the single soliton formation time and T_S is the time interval in which the pulse propagation is approximately solitonic.

rected by dissipation, and can increase from a value of $\pi/2$ (for $\Gamma=0$) up to π . The areas of pulses necessary for the formation of higher order solitons ($n>1$) are only weakly affected by dissipation since κ_n increases rapidly with increasing soliton number n .

The threshold expressions for envelope soliton formation in the dissipative medium, Eqs. (23) and (26), were experimentally confirmed for both purely dipolar spin waves propagating in tangentially magnetized YIG films^{23,24} (BVMSW) and for dipole-exchange spin waves propagating in perpendicularly magnetized YIG films.²⁶

All the above results apply to fully formed envelope solitons. It is, however, well-known that, if an input pulse of arbitrary (nonsolitonic) shape enters a nonlinear dispersive medium, a certain propagation time (or propagation distance) is necessary to form a soliton out of this input pulse. We propose to use the characteristic dissipation properties of an envelope soliton (i.e., the decay of its peak amplitude with a rate twice as large as for a linear cw signal) to determine experimentally the propagation times and distances where a single envelope soliton has been formed. This idea was previously suggested in Ref. 21 and successfully used in soliton collision experiments.¹⁸ There are also other opinions on this subject. For example, the authors of Ref. 11 proposed to use the symmetry of the output pulse profile as an indication that a soliton is fully formed. The symmetry criterion, however, is a qualitative one, and, in general, it is very difficult to check it experimentally, while the formation criterion based on the dissipative behavior of envelope solitons can be easily applied.

To illustrate our ideas about the soliton formation time we present a qualitative picture of evolution of a high-amplitude wave packet propagating in a nonlinear dispersive medium with dissipation in Fig. 3. The packet with initial amplitude U_0 and duration T_0 is excited at $t=0$. This packet propagates in the medium subject to the combined influence of nonlinearity, dispersion, and dissipation. After a characteristic propagation time T_F this pulse is reshaped and turned into a solitonic pulse with the amplitude U_{\max} and duration T . The solitonic pulse then propagates in the medium for a time T_S . During this time the shape of the pulse envelope remains solitonic (i.e., sech-like) but its amplitude decreases and its

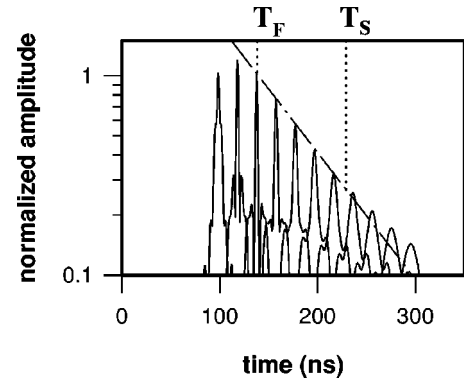


FIG. 4. Profiles of approximately solitonic pulses numerically calculated from Eq. (1) for the parameters of the experiment (Ref. 10) and rectangular input pulses of duration $T=15$ ns. The initial amplitude of the input pulse was chosen such that the pulse area corresponds to the upper boundary of the single-soliton regime [$n=2$ in Eqs. (3) and (16)]. The soliton formation time T_F is defined as a propagation time at which propagating pulse starts to demonstrate “solitonic” dissipation [see Eq. (19)].

width increases because of dissipation. At $t=T_F+T_S$ the pulse amplitude has decreased to U_{\min} defined by Eq. (25). Then the nonlinearity becomes insufficient to compensate the dispersion spreading of the wave packet, and the solitonic pulse turns into an ordinary linear pulse. The amplitude of the linear pulse decreases monotonously on propagation due to dispersion spreading and damping. It is this “approximately solitonic” nonlinear wave packet moving in the limited interval of propagation times $T_F < t < T_F+T_S$ that is usually called “envelope soliton” in a dissipative medium. Thus, the dissipation in the medium not only influences the threshold of soliton formation [see Eqs. (23) and (25)], but also limits the time interval (both from above and from below) in which nonlinear wave packets can propagate in a dissipative medium as solitons. A theoretical estimate of the single-soliton formation time T_F is given below.

Numerical calculations of T_F in terms of the NSE model (1) in the case without dissipation ($\Gamma=0$) were reported in Ref. 27. The soliton formation time T_F was defined in Ref. 27 as the moment when the amplitude of the propagating pulse stops to change and remains constant. Thus the formation time T_F for a rectangular ($\beta=1$) input pulse, having an initial amplitude and duration such that the area of the pulse corresponds to $n_{\text{eff}}=3/2$ ($N_S=1$), turned out to be proportional to the dispersion time T_D , $T_F=BT_D$ with the proportionality coefficient $B \approx 2.5$.

In the dissipative case ($\Gamma \neq 0$) we suggest to use Eq. (23) to define a new characteristic time $T_{\Gamma D}$ (*dispersion time in a dissipative medium*) as the inverse of the right-hand-side part of Eq. (23) for $n_{\text{eff}}=3/2$ ($N_S=1$):

$$T_{\Gamma D} = \frac{|D|\kappa_{3/2}^2}{\Gamma^2 + \frac{1}{4}D^2\kappa_{3/2}^4}. \quad (28)$$

This definition can be rewritten entirely in terms of the characteristic times T_D and T_Γ [see Eqs.(12) and (20)]:

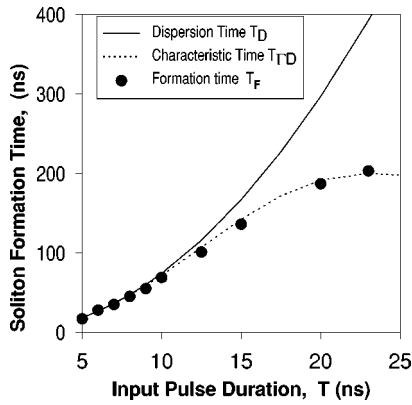


FIG. 5. Characteristic times of a single envelope soliton formation as functions of the input rectangular pulse duration T . Solid line: dispersion time T_D calculated using Eq. (11); broken line: characteristic time $T_{\Gamma D}$ calculated from Eq. (28); full circles: numerically calculated soliton formation time T_F determined as in Fig. 4. All model parameters are as in Fig. 4 and in experiment (Ref. 10).

$$T_{\Gamma D} = \frac{T_D}{1 + (T_D/2T_\Gamma)^2}. \quad (29)$$

It is reasonable to assume that $T_{\Gamma D}$ would be a good analytical estimate for the formation time of a single soliton in a dissipative medium: $T_F \approx T_{\Gamma D}$, similar to T_D being a good estimate of the formation time in a medium without dissipation. Note that from Eqs. (23) and (29) it follows that for a single ($N_S=1$) soliton we have $T_{\Gamma D}=T_N$. It is also clear from Eq. (29) that $T_{\Gamma D} < T_D$. Consequently, in a *dissipative* ($\Gamma \neq 0$) medium a fundamental ($N_S=1$) envelope soliton is formed *faster* than in the medium without dissipation.

To evaluate the quality of the theoretical estimate, Eq. (29), for the soliton formation time T_F , it is necessary to use some criterion for the soliton formation in a *dissipative medium*. The best choice is the criterion suggested in Ref. 21 based on the property of the fully developed soliton to dissipate exponentially twice as fast as a linear cw signal. Thus, the soliton formation time T_F in a ferrite film is the propagation time at which the solitonic dissipation starts.

Figure 4 shows a numerical simulation of the profiles of solitonlike pulses formed from an initial rectangular pulse of duration $T=15$ ns after different propagation times. The initial amplitude of the pulse was chosen in such a way that the pulse area corresponds to the upper boundary of the single-soliton regime [$n=2$ in Eqs. (3) and (16) and in Fig. 2]. The typical parameters of spin-wave soliton experiments¹⁰ $v_g = -3.2$ cm/ μ s, $D = 1.4 \times 10^3$ cm²/s, and $\Gamma = 5 \times 10^6$ s⁻¹ were used in this calculation. It can be seen in Fig. 4 that within the time interval $T_F < t < T_S$ the attenuation of the propagat-

ing pulse is solitonic, i.e., linear in a logarithmic scale, and, thus, T_F can be considered as the numerically calculated *soliton formation time*. T_F was evaluated for different values of the input pulse duration T (while the area of the input pulse corresponding to $n=2$ was kept constant) using graphs similar to the ones shown in Fig. 4. The characteristic times T_D and $T_{\Gamma D}$ were calculated for the same parameters of the NSE (1) and different values of T using Eqs. (12) and (29). The numerical results of all these calculations presented in Fig. 5 clearly demonstrate that in a dissipative medium, the single soliton formation time T_F indeed becomes smaller than that in a medium without dissipation. We can conclude from Fig. 5 that $T_{\Gamma D}$ yields a reasonable quantitative estimate of the numerically determined formation time T_F . Preliminary measurements of the BVMSW soliton formation time²⁸ (defined as suggested above) performed in a weakly dissipative YIG waveguide also gave a value of T_F that is substantially smaller, than the characteristic dispersion time T_D . The result²⁸ qualitatively supports the above proposed expression for the soliton formation time in a dissipative medium Eq. (29), but additional experimental investigations are necessary to check the quantitative validity of the formula (29).

VI. CONCLUSION

The analytical and numerical results presented above show that dissipation plays an important qualitative role in the process of formation and propagation of solitonic pulses in weakly dissipative media. In ferrite waveguides where the influence of dissipation is much stronger than in optical fibers, dissipation should always be taken into account since it determines the minimum threshold of envelope soliton formation and the shape of the threshold curve for soliton formation. The characteristic solitonic dissipation of the peak power of the wave packet propagating in a dissipative medium can be used to determine experimentally the time when the propagating wave packet becomes a fully formed “approximate” envelope soliton. This formation time can be estimated analytically including the effects of dissipation. All these conclusions are well supported by the numerical modeling in the framework of the NSE model, and most of them are also supported by our laboratory experiments performed on both dipole-dominated (BVMSW) and dipole-exchange spin waves propagating in YIG film waveguides.

ACKNOWLEDGMENTS

The authors are grateful to Professor B.A. Kalinikos and Professor Yu.K. Fetisov for many helpful discussions. This work was supported in part by the NSF Grants No. DMR-0072017 and No. INT-0072017, by the Oakland University Foundation, and by the DFG Grant No. BE 864/1.

¹G.P. Agrawal, *Nonlinear Fiber Optics*, 2nd ed. (Academic Press, San Diego, 1995), Chap. 5.

²*Optical Solitons: Theory and Experiment*, edited by J.R. Taylor (Cambridge University Press, Cambridge, 1992), Chap. 3.

³*Nonlinear Phenomena and Chaos in Magnetic Materials*, edited by P.E. Wigen (World Scientific, Singapore, 1994), Chap. 9.

⁴A.N. Slavin, *J. Phys. IV* 7, C1-379 (1997).

⁵*Solitons in Action*, edited by K. Lonngren and A. Scott (Academic

- Press, New York, 1978).
- ⁶V.E. Zakharov and A.B. Shabat, Zh. Éksp. Teor. Fiz. **61**, 118 (1971) [Sov. Phys. JETP **34**, 62 (1972)].
- ⁷O. Buettner, M. Bauer, S.O. Demokritov, B. Hillebrands, Yu. Kivshar, V. Grimalsky, Yu. Rapoport, and A.N. Slavin, Phys. Rev. B **61**, 11 576 (2000).
- ⁸S.O. Demokritov, B. Hillebrands, and A.N. Slavin, Phys. Rep. **348**, 535 (2001).
- ⁹M.J. Lighthill, J. Inst. Math. Appl. **1**, 269 (1965).
- ¹⁰M. Chen, M.A. Tsankov, J.M. Nash, and C.E. Patton, Phys. Rev. B **49**, 12 773 (1994).
- ¹¹A.D. Boardman, S.A. Nikitov, K. Xie, and H. Mehta, J. Magn. Magn. Mater. **145**, 357 (1995).
- ¹²Yu.S. Kivshar, J. Phys. A **22**, 337 (1989).
- ¹³J. Burzlaff, J. Phys. A **21**, 561 (1988).
- ¹⁴A. Hasegawa and Y. Kodama, Proc. IEEE **69**, 1145 (1981).
- ¹⁵B.A. Kalinikos, N.G. Kovshikov, and A.N. Slavin, Zh. Éksp. Teor. Fiz. **94**, 159 (1988) [Sov. Phys. JETP **67**, 303 (1988)].
- ¹⁶M.A. Tsankov, M. Chen, and C.E. Patton, J. Appl. Phys. **76**, 4274 (1994).
- ¹⁷B.A. Kalinikos and N.G. Kovshikov, Pis'ma Zh. Éksp. Teor. Fiz. **60**, 290 (1994) [JETP Lett. **60**, 305 (1994)].
- ¹⁸N.G. Kovshikov, B.A. Kalinikos, C.E. Patton, E.S. Wright, and J.M. Nash, Phys. Rev. B **54**, 15 210 (1996).
- ¹⁹J. Satsuma and N. Yajima, Prog. Theor. Phys. Suppl. **55**, 284 (1974).
- ²⁰T. Komukai, T. Yamamoto, T. Sugawa, and Y. Miyajima, Electron. Lett. **28**, 830 (1992).
- ²¹B.A. Kalinikos, N.G. Kovshikov, and A.N. Slavin, IEEE Trans. Magn. **28**, 3207 (1992).
- ²²H. Xia, P. Kabos, C.E. Patton, and H.E. Ensle, Phys. Rev. B **55**, 15 018 (1997).
- ²³J.M. Nash, C.E. Patton, and P. Kabos, Phys. Rev. B **51**, 15 079 (1995).
- ²⁴A.N. Slavin, Phys. Rev. Lett. **77**, 4644 (1996).
- ²⁵V.S. L'vov, *Wave Turbulence Under Parametric Excitation* (Springer, Berlin, 1994), p. 28.
- ²⁶A.N. Slavin, H. Benner, K.J. Foos, and T. Lesperance, J. Phys. IV **7**, C1- 459 (1997).
- ²⁷R.A. Staudinger, P. Kabos, H. Xia, B.T. Faber, and C.E. Patton, IEEE Trans. Magn. **34**, 2334 (1998).
- ²⁸Yu.K. Fetisov, A.N. Slavin, and T. Lesperance, J. Appl. Phys. **81**, 4313 (1997).